LSSVM Model for Penetration Depth Detection in Underwater Arc Welding Process

WeiMin Zhang [1, 2+], GuoRong Wang [1], YongHua Shi [1] and BiLiang Zhong [1]

[1] South China University of Technology, Guangzhou, 510640, PR China
[2] Guangzhou Maritime College, Guangzhou, 510725, PR China

Abstract. For underwater arc welding, it is much more complexity and difficulty to detect penetration depth than land arc welding. Based on least squares support vector machines (LSSVM), welding current, arc voltage, travel speed, contact-tube-to-work distance, and weld pool width are extracted as input units. Penetration depth is predicted in underwater flux-cored arc welding (FCAW). For improvement prediction performance, the LSSVM parameters are adaptively optimized. The experimental results show that this model can achieve higher identification precision and is more suitable to detect the depth of underwater FCAW penetration than back propagation neural networks (BPNN).

Keywords: underwater arc welding, penetration depth, least squares support vector machines

1. Introduction

The weld penetration depth can mainly represent the weld quality in weld bead geometry (penetration depth, bead height, and weld pool width) [1]. If the defective weld penetration occurrences can be recognized in time, the weld quality can be monitored on-line. For land arc welding, some reports can be found on monitoring welding quality through penetration depth detecting. For underwater arc welding, it is very hard to detect the depth of penetration real-time, ascribed to the invisibility of welding process. Up to now, there is no research report on this technique in underwater arc welding, due to its more complexity and difficulty than land arc welding. Nevertheless, the underwater arc welding technique plays a critical role in construction and maintenance of ships, dockyards, port facilities, and ocean terrace etc [2]. As one of gas metal arc welding, flux-cored arc welding (FCAW) is suitable for underwater arc welding. In this paper, penetration depth detecting in underwater FCAW is investigated in detail. In order to set up a guideline for penetration depth detection from the multi-sensor data fusion model, the welding process variables are systematically and quantitatively analyzed on their influence on depth of penetration and weld pool width through underwater FCAW experiment. Because of hard environment in underwater FCAW, it is difficulties to get enough training sample sets for penetration depth prediction. Suggested by Suykens [3-4], the least squares support vector machines (LSSVM) is more suitable for non-linearity function prediction with a reasonably small size of training sample sets. With higher performance of predication than back propagation neural networks (BPNN), LSSVM has been very successfully applied in pattern recognition, non-linear function estimation, and machine learning domains, etc [3-6]. Hence, the LSSVM is introduced into penetration depth prediction modeling in underwater FCAW. In this model, the radial basis function (RBF) is selected as kernel function and the LSSVM parameters are adaptively optimized to improve prediction performance.

2. Methodology

Underwater FCAW is a complex heat transfer process. The formation of underwater welding pool is interacted by electric field, magnetic field, and flow field. The study showed that the depth of penetration was mainly affected by heat-transfer energy of workpiece [7]. Moreover, the workpiece thermal energy is mainly affected by some underwater welding process variables, such as welding current, travel speed, arc

---

[+] Corresponding author. Tel.: +86-020-82384979.
E-mail address: super208956@163.com.

voltage, and contact-tube-to-work distance (CTWD). Suppose the penetration depth is P, welding current is I, arc voltage is U, travel speed is S, and CTWD is H. Based on multi-sensor data fusion model, P can be represented as

$$P = f(I, U, S, H) \qquad (1)$$

In addition, there is a relationship between the penetration depth and the weld pool width at certain time and welding condition. Combined with the information of weld pool width, the detected result of penetration depth will be more reliable. Thus, the depth of penetration at certain time can be predicted as

$$P = f(I, U, S, H, W) \qquad (2)$$

where W is the weld pool width. In this study, welding current I, arc voltage U, and weld pool width W will be acquired and analyzed from welding current sensor system, arc voltage sensor system, and laser structured vision sensor system. Meanwhile, travel speed S and CTWD H can be confirmed and inputted. With the higher performance of predication than BPNN, LSSVM is selected as multi-sensor data fusion model [3-6].

3. Experiment and analysis

3.1. Experiment

The LSSVM prediction model of relationships between penetration depth and welding process variables must need to be established accurately. Thus, the sufficient experimental data must be provided for prediction model training and verifying [8].

Conducted the bead-on-plate welding, the experimental materials were 140mm× 40mm × (6～10)mm A3 low-carbon steel plates. In this study, the chosen welding process variables were welding current, arc voltage, travel speed, and CTWD. The SQJ501 is used as the flux-cored wire with a diameter of 1.6 mm. And the Dimension of water tank is 15000 mm× 600mm × 500mm. Positioned in a plane 100mm deep water, the workpiece welding procedure is performed. Under the bounds of welding process variables, the optimum weld geometry could be formed.

Travel speed and CTWD are confirmed for the same workpiece during underwater FCAW process. Meanwhile, welding current, arc voltage, and weld pool width are detected and recorded in time. For different workpiece, at least one of these parameters is variable. At one time of underwater FCAW process, welding current, travel speed, CTWD, arc voltage and weld pool width are obtained as input data of trial model. To measure the penetration depth, the bead section was cut transversely from the middle position using the wire cutting machine. To assure the precision of the specimen dimension, it was etched by HNO_3 3% and H_2O 97%. Hence, the actual penetration depth at corresponding time is measured after welding and selected as output data of trial model.

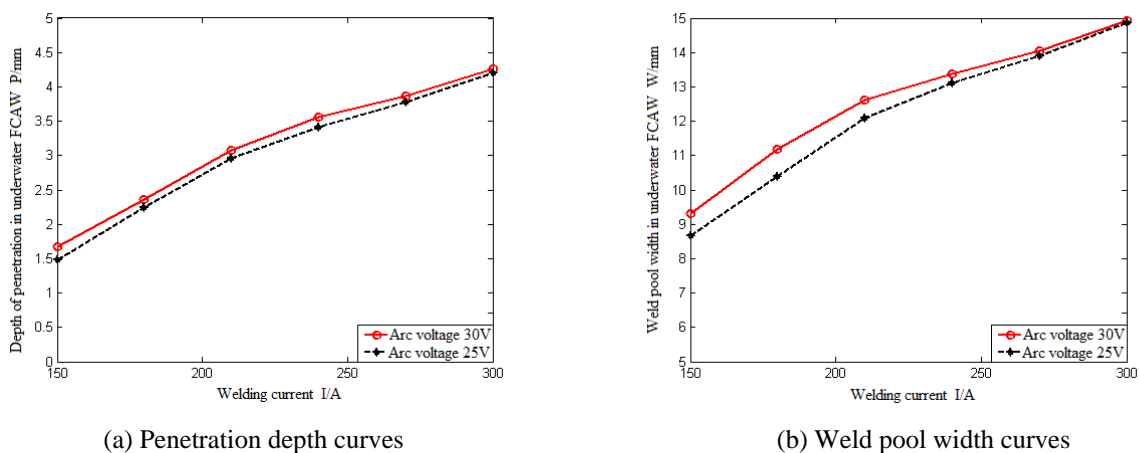### 3.2. Effects of the welding current and arc voltage on penetration depth and weld pool width

| (a) Penetration depth curves | (b) Weld pool width curves |

Fig. 1: Penetration depth and weld pool width with welding current and arc voltage variable.

(a) Penetration depth curves   (b) Weld pool width curves
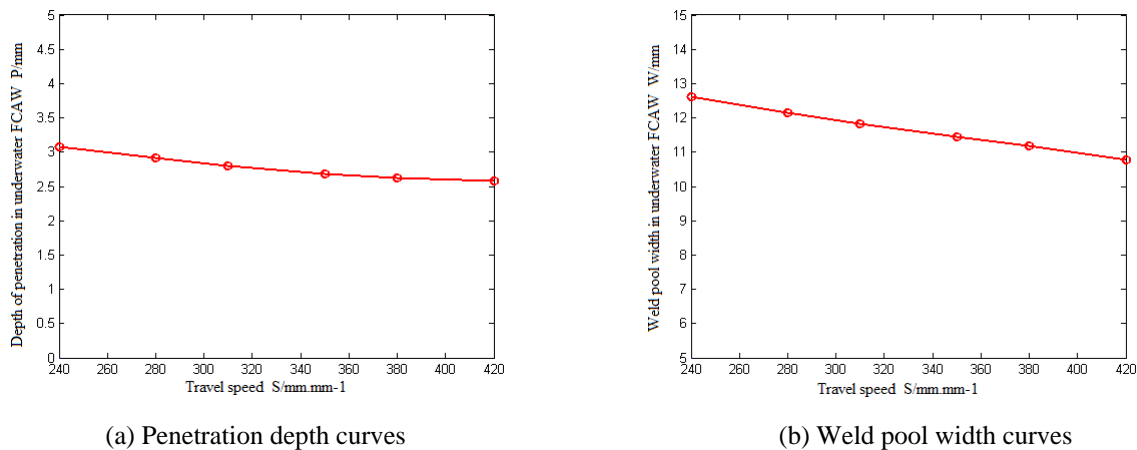
Fig. 2: Penetration depth and weld pool width with travel speed variable.

With 240 mm•min-1 travel speed and 18 mm CTWD, true penetration depth and weld pool width curves for different welding currents at 25V and 30V arc voltage are shown in fig.1. With very significant effect, it is evident that an increase in welding current results in increased penetration depth and weld pool width at all levels of arc voltage. Thus, welding current is the first parameter to be considered for decreasing penetration depth and weld pool width. With less influence than welding current, there is an increase in penetration depth and weld pool width with an increase in arc voltage. This is due to the fact that, at higher welding current and arc voltage, the fusion rate becomes higher with higher fluidity of the molten wire and causing larger weld pool. Therefore welding current can assist in penetration depth control.

3.3. Effect of the travel speed on penetration depth and weld pool width

With 210A welding current, 30V arc voltage and 18 mm CTWD, the true penetration depth and weld pool width curves for variable travel speed are shown in fig.2. From fig. 2, it can be observed that there is a decrease in penetration depth and weld pool width with an increase in travel speed. But the effect is not very significant. This may be due to the fact that, if the welding speed is increased, the weld pool becomes smaller, penetration depth and weld pool width decrease, but only to a certain limit.

3.4. Effect of the CTWD on penetration depth and weld pool width

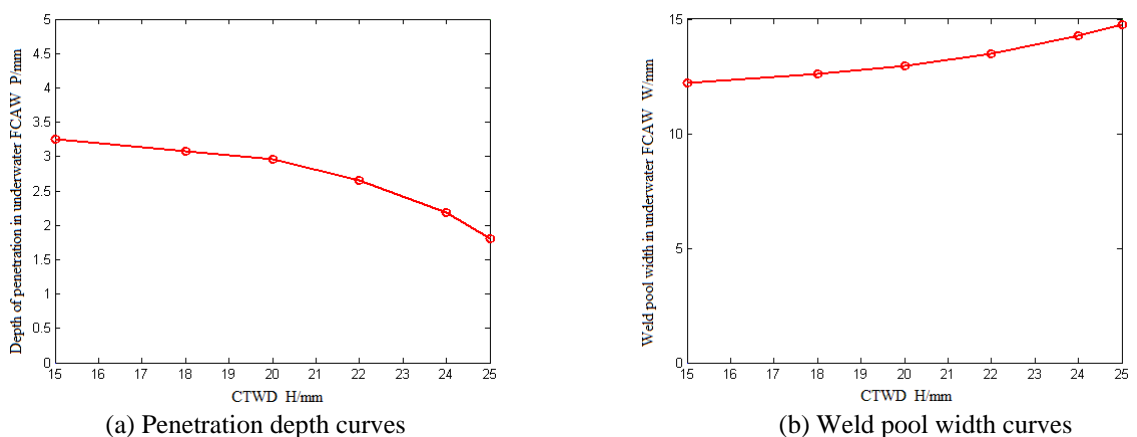(a) Penetration depth curves   (b) Weld pool width curves

Fig. 3: Penetration depth and weld pool width with CTWD variable.

Fig.3 shows the true penetration depth and weld pool width curves with different CTWD at 210A welding current, 30V arc voltage and 240 mm•min-1 travel speed welding condition. Though the CTWD does not have much influence on penetration depth and weld pool width, compared to welding current. It can be seen from fig.3 (a), if the CTWD is increased, that at the beginning of the drawing the depth of

penetration decreases a little and then sharply diminishes. On the contrary, it can be seen from fig.3 (b) that the weld pool width first increases a little and then increases more with the further increase of CTWD. Lower fusion rate may be attributed for this decrease in penetration depth and increase in weld pool width with an increase in CTWD.

4. The LSSVM model of adaptive optimizing parameters

Introduced for nonlinear function estimation, LSSVM can be used to predict the depth of penetration in underwater FCAW process [3-4].

Suppose we are given a set of N training data points $\{x_i, y_i\}_{i=1}^N$, where $x_i \in R^n$ denotes the input space of the sample and has a corresponding target value $y_i \in R$ for $i = 1, \ldots, N$. The non-linear function estimation modelling takes the form as:

$$y(x) = w^T \varphi(x) + b \tag{3}$$

where $\varphi(x)$ denotes the high dimensional feature space which is nonlinearly mapped from the input space, w is the weight vector and b is the bias term. Then, in the framework of empirical risk minimization the cost function is formulated

$$\min J(w,e) = \frac{1}{2} w^T w + \frac{1}{2} \gamma \sum_{i=1}^N e_i^2 \tag{4}$$

subject to the equality constrains

$$y_i(x) = w^T \varphi(x_i) + b + e_i, i = 1, \ldots, N \tag{5}$$

where e_i is the random errors and γ is a regularization parameter in determining the trade-off between minimizing the training errors and minimizing the model complexity. Important differences with standard SVM are the equality constrains and the squared error term, which greatly simplifies the problem.

For solving this optimization problem, The Lagrange function is constructed

$$L(w,b,e,a) = J(w,e) - \sum_{i=1}^N a_i \left\{ w^T \varphi(x_i) + b + e_i - y_i \right\} \tag{6}$$

where $a_i \in R$ are the Lagrange multipliers. The conditions for optimality solution can be obtained by partially differentiating with respect to w, b, e_i and a_i

$$\begin{cases} \dfrac{\partial L}{\partial w} = 0 \rightarrow w = \sum_{i=1}^N a_i \varphi(x_i) \\ \dfrac{\partial L}{\partial b} = 0 \rightarrow \sum_{i=1}^N a_i = 0 \\ \dfrac{\partial L}{\partial e_i} = 0 \rightarrow a_i = r e_i \\ \dfrac{\partial L}{\partial a_i} = 0 \rightarrow w^T \varphi(x_i) + b + e_i - y_i = 0 \end{cases} \tag{7}$$

After elimination of e_i, w, the following linear equation can be obtained:

$$\begin{bmatrix} 0 & \vec{1}_N^T \\ \vec{1}_N & \varphi(x_i)^T \varphi(x_j) + r^{-1} I_N \end{bmatrix} \begin{bmatrix} b \\ a \end{bmatrix} = \begin{bmatrix} 0 \\ y \end{bmatrix} \tag{8}$$

where $y = [y_1; \ldots; y_N]^T$, $\vec{1}_N = [1; \ldots; 1]^T$, $a = [a_1; \ldots; a_N]^T$, I_N is an $N \times N$ identity matrix, and the Mercer condition has been applied

$$\Omega_{ij} = \varphi(x_i)^T \varphi(x_j) = K(x_i, x_j), \quad i, j = 1, \ldots, N \tag{9}$$

where $\Omega \in R^{N \times N}$, $K(x_i, x_j)$ is defined as kernel function.

Finally, the parameters a_i, b are based on the solution to (8). As seen in fig.4 , LSSVM model regression can be expressed as [3-4]:

$$y(x) = \sum_{i=1}^{N} a_i K(x_i, x) + b \tag{10}$$

where $x = [x_1, x_2, \cdots, x_l]^T$ denotes the input vector of independent variables, N is the size of data point sets, y is the corresponding output, a_i is the Lagrange multiplier and b is the bias term.

In comparison with some other feasible kernel functions, the radial basis function (RBF) is selected as kernel function due to its good features [9]. We employ kernel function with the form

$$K(x_i, x) = \exp(-\|x - x_i\|^2 \sigma^{-2}) \tag{11}$$

The width of kernel σ is a positive real constant. There are only two additional parameters to be tuned σ and γ, which determine the trade-off between minimizing the training errors and minimizing the model complexity. If σ and γ parameters are selected as finite candidate tuning sets, k-folds cross validation is a popular technique for certain optimization parameters (γ, σ) [6]. However, the prediction error accuracy of this trial may not be satisfied. For improving the generalization performance and prediction accuracy, an adaptive optimizing parameter method is proposed. The test prediction error of this trial can be calculated by the following equation:

$$MSE = \frac{1}{N} \sum_{i=1}^{N} [y(i) - f(i)]^2 \tag{12}$$

where MSE is the mean square error, $y(i)$ and $f(i)$ are the prediction and actual value respectively, N is the size of the test subsets.
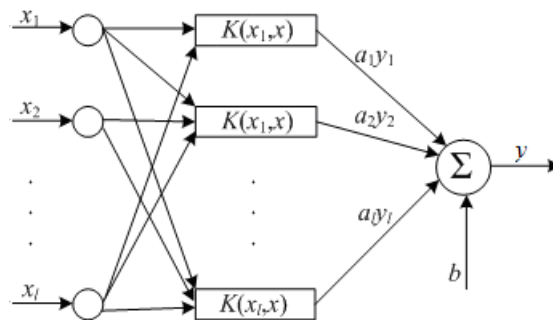

Fig. 4: LSSVM model structure.

Suppose averaged set of l training data points $\{x_i, y_i\}_{i=1}^l$ by k, where $x_i \in R^n$ denotes the n dimension input space of the sample and has a corresponding target value $y_i \in R$ for $i = 1, 2, \cdots, l$. ξ_0 is satisfaction MSE, $\xi_{\min}$ is minimum MSE for every certain (γ, σ), $L_{\max}$ is the training steps, $\sigma_{\max}$ is the maximum of σ, and $\gamma_{\max}$ is the maximum of γ. The proposed adaptive parameter optimization procedure for LSSVM is described as follows:

Step 1: Input $\{x_i, y_i\}_{i=1}^l, \xi_0, k, \gamma_{\max}, \sigma_{\max}, L_{\max}, L = 0$.

Step 2: $L = L + 1$.

Step 3: Cross combination (γ_i, σ_j)

$$\gamma_i = 0.1 + \frac{i(\gamma_{\max} - 2^{-L})}{L}(i = 0, \cdots, L); \sigma_j = 0.01 + \frac{j(\sigma_{\max} - 2^{-L})}{L}(j = 0, \cdots L).$$

Step 4: k - folds cross validation for certain parameters (γ_i, σ_j).

Step 5: Go to step 3 until it has implemented $(L+1) \times (L+1)$ generations.

Step 6: Calculate $\xi_{\min} = \min \xi_i (i = 1, \cdots, (L+1) \times (L+1)$, reserve $\xi_{\min}$ and corresponding (γ, σ).

Step 7: If $\xi_{\min} \geq \xi_0$ and $L_{\max} \geq L$, go to step 3.

Step 8: Obtain certain optimizing parameters (γ, σ).

Finally, the LSSVM model of adaptive optimizing parameters is set up for penetration depth prediction in underwater FCAW.

5. Results and Verification

In the underwater FCAW experiment, welding current, arc voltage, travel speed, CTWD, and weld pool width are selected as input units. Because of heat inertia, the currently and three-before time welding current, arc voltage and weld pool width are all obtained as inputs [10]. Finally, the total 14 input units are $I(t), I(t-1), I(t-2), I(t-3), U(t), U(t-1), U(t-2), U(t-3),\quad W(t), W(t-1), W(t-2), W(t-3)$, $S(t)$ and $H(t)$. Meanwhile, the one output is penetration depth $P(t)$.

Table 1 Compare the prediction performance between BPNN and LSSVM.

Prediction model	MSE	$MaxAE$	$MeanAE$	T_{CT} (s)
BPNN	0.010	0.34	0.07	2457.26
LSSVM	0.003	0.40	0.03	1125.70

In this study, cross validation is averaged by four, $L_{\max}$ is 50,000, ξ_0 of MSE is 0.004, $\gamma_{\max}$ is 1000, and $\sigma_{\max}^2$ is 100. Using adaptive optimizing parameter method, the optimization parameters (γ, σ) are obtained. Given the original data point sets, the LSSVM model is established. The test prediction error of validation data point sets and modelling time are listed in table 1. The $MaxAE$ (Maximum Absolute Error) and the $MeanAE$ (Mean Absolute Error) are calculated by following equations:

$$MaxAE = \max_{i=1}^{N} \| [y(i) - f(i)] \| \tag{13}$$

$$MeanAE = \frac{1}{N} \| [y(i) - f(i)] \| \tag{14}$$

where $y(i)$, $f(i)$ and N are the same as (5). The T_{CT} is the modelling time. In addition, the BPNN model is introduced to compare the performance of this LSSVM model. The non-linear activation function of BPNN is the sigmoid function

$$f(x) = \frac{1}{1 + \exp(-x)} \tag{15}$$

The optimized BPNN structure is 14-12-1 three layers network. The BPNN algorithm with momentum is chosen as algorithm of gradient method, and the training rate is 0.5, the momentum factor is 0.3 [10]. For the same original data point sets, cross validation is also averaged by four, and the training steps are 50,000 to confirm BPNN parameters. In order to compare the performance of prediction model, the test prediction error of validation data point sets and modelling time are also listed in table 1. Moreover, the error curves of the prediction and actual value for validation data point sets are shown in fig.5 to compare prediction precision between LSSVM and BPNN.
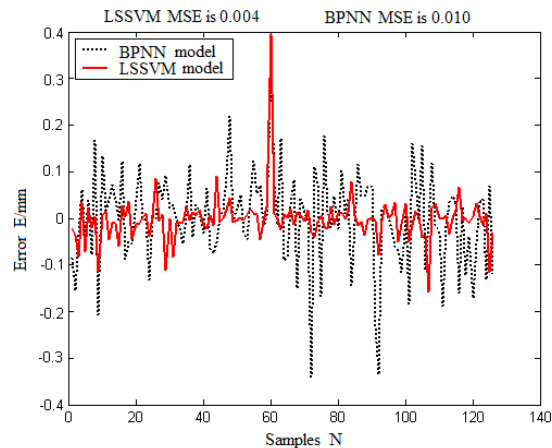
Fig. 5: Prediction error results of penetration depth.

Except *MaxAE* for LSSVM model in table 1, the other results of test prediction error are all better and the modelling time is less than BPNN model. Also, prediction error of LSSVM is usually less than BPNN in fig.5. Because of strong non-linear characteristics, a lot of training data samples must be required to establish BPNN model in underwater FCAW. Fewer training data will cause neutral network learning not enough. But the LSSVM algorithm is suitable for small data samples learning. Further more, the prediction error accuracy is assured and the complexity of computation is reduced by the proposed adaptive optimizing parameter method. Compared with BPNN, the identification precision and modelling efficiency are all improved.

6. Conclusion

Represented by weld penetration depth, the weld quality is successfully detected with LSSVM model in underwater FCAW. In order to evaluate the penetration depth, the effects of underwater welding process variables on penetration depth and weld pool width are analyzed. The parameters γ and σ of LSSVM are adaptively optimized to avoiding the unsatisfied prediction error accuracy. As a result, the depth of penetration can be detected effectively. Experimental analysis proves that this model can obtain higher prediction performance and is more suitable for penetration depth detection than BPNN in underwater FCAW.

7. Acknowledgements

8. References

[1]   B. S. Sung, I. S. Kim, Y. Xue, et al. Fuzzy regression model to predict the bead geometry in the robotic welding process. *Acta Metallurgica Sinica(English Letters)*. 2007, **20**(6):391-397.

[2]   A. P. Michale. Underwater wet welding became a viable option. *Welding & Fabrication*. 1998, **66**(6): 12-14.

[3]   J. A. K. Suykens, J. Vandewalle. Least squares support vector machines classifiers. *Neural Processing Letters*. 1999, **9**(3):293-300.

[4]   J. A. K. Suykens, J. Vandewalle. Recurrent least squares support vector machines. *IEEE Trans. Circuits Systems-I*. 2000, **47**(7): 1109-1114.

[5]   J. A. K. Suykens, J. De Barbanter, and L. Lukas, et al. Weighted least squares support vector machines: robustness and sparse approximation. *Neurocomputing*. 2002, **48**(1-4): 85-105.

[6]   D. F. Shi, N. N. Gindy. Tool wear predictive model based on least squares support vector machines. *Mechanical Systems and Signal Processing*. 2007, **21**: 1799-1814.

[7]   M. A. Wahab, M. J. Painter, and M. H. The prediction of the temperature distribution and weld pool geometry in the gas metal arc welding process. *Journal of Materials processing technology*. 1998, **77**: 233-239.

[8]   C. S. Wu, J. Q. Gao, and Y. H. Zhao. A neural network for weld penetration control in gas tungsten arc welding. *Acta Metallurgica Sinica(English Letters)*. 2006, **19**(1): 27-33.

[9]   J. C. Patra, A. V. D. Bos. Modeling of an intelligent pressure sensor using functional link artificial neural networks. *ISA Transactions*. 2000, **39**: 15-27.

[10] S. B. Chen, Y. Zhang, and T. Qiu, et al. Robotic welding systems with vision-sensing and self-learning neuron control of arc welding dynamic process. *Journal of Intelligent and Robotic Systems*. 2003, **36**: 191-208.